Structural assessment based on photogrammetry measurements and finite element method

A. Cubells Barceló

Insituto Superior Técnico, Lisboa

The objective of the present study is to develop a new approach to model the initial geometrical imperfections of ship plates by using the analytical photogrammetry. This technique is able to take measurements of the distortions of plates and to catch the dominant surface shape, including the out-of-plane of the edges and the asymmetries. Having this data, it is possible to generate faithful models of plates based on third order polynomial functions. Finally, the maximum load-carrying capacity of the plates can be analysed by performing a nonlinear finite element analysis using a commercial finite element code. Seven plates, three un-stiffened and four stiffened, have been modelled and analysed in this study. For each plate, two initial imperfection models have been generated: one, based on photogrammetric measurements and the other, based on the trigonometric Fourier functions. Both models are subjected to the same uniaxial compressive load and boundary conditions in order to study the behaviour through the strength-strain response curves. The present work also studies the use of the photogrammetry to measure the level of corrosion degradation depth of steel plates. Relying on the stereographic photographs, a dense cloud of points modelling the roughness of the surface of plates is generated and the points' dispersion is used to compute the corrosion depth.

1. INTRODUCTION

Ship structures are predominantly made of steel plates and stiffeners forming panels. They have widely been used as primary structural components due to the simplicity of fabrication and their high strength-weight ratio. During the service lifetime, these panels are subjected to axial loads and bending moment stresses making the structure susceptible to failure. One of the major stability losses is due to buckling of plates, which are part of stiffened panels. Nowadays there is still insufficient knowledge about their behaviour. In order to evaluate the capacity of the plates, the Ultimate Limit State is used.

The analysis of the ultimate strength of ship structures, taking into account all possible failure modes -plate induced overall buckling (PI), stiffened induced overall buckling (SI), stiffener tripping (ST) and plate buckling (PB) is not trivial because of the interaction of various factors such as geometry and material properties: loading, boundary conditions, residual stresses and post-weld out-of-plane initial imperfections. The material, with which ship plates are commonly made, is mild or high tensile steel and they can be square or rectangular. The loads might be considered in-plane loading, distributed lateral load due to water pressure or the combination of both. The boundary conditions are related to the design of the structure and depend on the position of the plate inside of the structure. The latter factor, the out-of-plane initial imperfections, is the principal factor to be evaluated in this study while the residual stresses are not approached inheres.

The initial imperfections are generated by production processes such as welding, manoeuvring, cutting and so forth and their influence is of high relevance. During the years, many authors such as Carlsen (1978), Guedes Soares (1988), Frankland (1940)andSmith (1979), have been studied how the ultimate strength of a plate is affected by the presence of initial imperfections, proposing design methods and equations to predict the ultimate strength. Karman and Sechler (1932) proposed an equation relating the ultimate strength and the plate slenderness,

$$\beta = \frac{b}{t}\sqrt{\frac{\sigma_0}{E}} \tag{1}$$

Frankland (1940), introduced quadratic terms to the former equation and Gerard modified the equation in 1957 to characterize plates with plastic behaviour. Finally, Faulkner (1975), proposed a formula for simply supported plates with elasto-plastic behaviour that became one of the most widely used equations on marine structures. Faulkner also found that the presence of the residual stresses reduces the compressive strength by as much as 20% and that the relationship between the non-dimensional amplitude of the initial distortions and the slenderness ratio may be defined as,

$$\phi_u^{Fa} = \begin{cases} 1, & if \beta \le 1 \\ \frac{2}{\beta} - \frac{1}{\beta^2} if \beta \le 1 \end{cases} \tag{2}$$

$$\left(\frac{W_{max}}{t}\right)_{Fa} = 0.10\,\beta^2 \tag{3}$$

Most of the research concerning the effect of welding distortions concentrates only on the maximum initial distortion amplitude, however, the evidence indicates that the welding distortion shape also significantly affects the ultimate compressive strength (Kamiski and Amadhl 2000).

A new formulation was proposed in order to divide the ultimate strength in various terms in an equation that considers two reduction parameters to the maximum ultimate strength,($\phi_{u=}\phi_u R_d R_r$).The first of these parameters regards the initial deflection and the second one, with the residual stresses due to welding. Across several years, the authors proposed formulas to evaluate the values for R_d and R_r such as Carlsen (1977), Guedes Soares (1988), and Cui (1988).

Among other authors, Dowling and Frieze (1977)alerted the fact that the first buckling mode was not necessary the worst scenario, being necessary to focus to the problem beyond the maximum initial deflection. Antoniou (1980) presented a study with 2000 measurements of plates were taken based on the principal mode of deflection. As a result, he proposed a new expression relating the initial deflections as a function of the plate slenderness,

$$\left(\frac{W_{max}}{t}\right)_A = 0.12\,\beta^2 \tag{4}$$

Carlsen (1978) analysed a typical "hungry horse" shape of initial imperfections in full-scale stiffened panels. This typical shape was found to have the same load-deflection curve with an initial imperfection pattern of three half-sine waves along the length of the plate and one half-sine wave cross across the width of the panel (Chi, Grondin et al. 2006).

Smith, Davidson et al. (1988) carried out an analysis of initial plate distortions of merchant ships concluding that the dominant distortion, mainly induced by the welding processes followed a sine wave form. He proposed three levels of initial residual stresses: slight, average and severe.

$$\left(\frac{W_{max}}{t}\right)_{Sm} = \begin{cases} 0.025\beta^2 Slight \\ 0.1\beta^2 Average \\ 0.3\beta^2 Severe \end{cases} \tag{5}$$

All the authors considered that the deformations of a plate might be expressed in Fourier expansion series as follows:

$$W_{0,exp} = \sum_{i=1} W_{0,i1} sin\left(\frac{i\pi x}{a}\right) sin\left(\frac{\pi y}{b}\right) \quad (6)$$

where$W_{0,i1}$ is the amplitude of the initial deflection. The number of terms that best represents the initial imperfections, as well as the amplitude of each of them, has been the milestone of the investigations along the years. Initially, it has been approached the initial geometrical imperfections is affecting only to the amplitude of deformation.

The models generated using this trigonometric function present two implicit characteristics, the first is that the edges of the plate will always be equal to 0, and hence, it is assumed that there are no deformations on the edges. The second characteristic is that, since the initial shape of the trigonometric model is symmetric, the response it is expected also to be symmetric in the displacements and stress distribution.

Guedes Soares and Gordo (1996) outlined that the initial geometry of the plate is very influential when the plate behaves inside of the pre-buckling regime, owed to the fact that the deformations are of less magnitude. They proved how determines the initial deformation mode and the maximum amplitude are, and show the importance of evaluating them.

Kamiski and Amadhl (2000) affirmed that the existing simplified methods might be not sufficiently good to achieve a more advanced buckling and ultimate strength design of ship plating, meaning that more sophisticated solution methods were needed. He outlined the increasing interest in the evolution of weld induced residual stresses and initial distortions. The prediction of UTS in design stages allows calculating more precisely the amount of strength degradation. Having this information, it is possible to identify favourable procedures that maximize the load carrying capacity of structures. In this sense, the present study is aimed to develop a procedure to predict accurately the initial distortions of steel plates and thus, the maximum capacity.

Herein has developed a methodology that, based on photogrammetric techniques, is able to generate faithful models of the plates to study. This methodology consists in: firstly, to get the coordinates of a certain number of points that belong to the surface of the plate through Photogrammetry, secondly, to generate a polynomial function that fit to those points, then, to use these mathematical functions to generate models that are similar to the real plates and finally, to carry out a non-linear structural analysis of the models based on Finite Element Method (FEM).

The proposed methodology is applied to model 7 specimens and the results are compared to those obtained from trigonometric models. The plates that belong to a girder box girderare specially treated so as to simulate the real characteristics of the plates found in marine structures. The set of specimens is composed by 3 un-stiffened plates plus 4 stiffened plates and the position they occupy in the whole structure is shown inFigure 1.

The aspect ratio of the most of them is approximately equal to 2 and thicknesses are measured by an ultrasonic gauge. All information is shown inTable 1. The elasticity modulus and the Poisson coefficient are considered to be of E = 206 GPa and $v = 0.3$ respectively.

Table 1 Specimens

Name	X *(a)*	Y *(b)*	a	Tk	b	W0 (0.12)	a/t
Plate4	175.9	341.6	1.9	2.70	2.5	2.10	65.1
Plate4_B	180.0	324.7	1.8	2.01	3.5	2.96	89.5
Plate7	176.1	327.0	1.9	2.02	3.4	2.82	87.2
Stiff3	189.5	334.2	1.8	2.90	2.6	2.27	65.3
Stiff4_B	180.0	323.9	1.8	2.90	2.4	2.05	62.1
Stiff7	175.1	322.3	1.8	2.50	2.7	2.25	70.0
Stiff 8	189.0	330.2	1.7	2.22	3.3	2.95	85.2

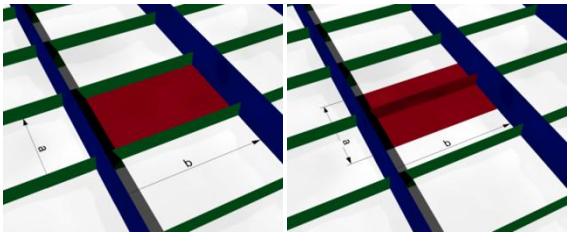

Figure 1 Un-stiffened (left) and stiffened (right) plates

2. PHOTOGRAMETRIC TECHNIQUES

Photogrammetry techniques have been used since 1800 when the idea of representing objects from images started to be attractive. One hundred years later, this technology has been applied in several areas, being predominant geological and terrestrial representations. More recently, the development of the technology permitted its application for close-range measurements when the size of the object to be measured and the camera-to-object distance are both less than 100m. Nowadays it is being used for measurements of medical, archaeological, architectural and industrial elements, as well as accident reconstruction.

In the following it is outlined some recent works in which the close-range technology is used successfully, showing out its potential in measuring processes. Koelman (2010) presented an industrial application of CAD that concerned the measurements and re-engineering of the shape of a complete ship hull and ship parts. In his study, he considered separately the 3D model measurements and the topological proprieties. Besides this, it was focused on modelling a large model scale and it was considered those cases where close-range study were needed such as ship repair phase, where measurements of flat constructions is a goal. Furthermore, in his work he presents a comparison between laser and photogrammetric techniques concluding that the latter is more appropriate for ship hull inverse engineering measurements.

Zaplatic (2008) also presented a procedure of dimensional and shape control of a sub-assembled section in shipbuilding based on photogrammetry. Such procedure allowed them to carry out a survey of the fabrication quality, being able to check out the flatness and the curvatures and compare the measured values with the CAD drawings. The importance of this quality control strives in the fact that inaccurate sub-assembled blocks in shipbuilding carry to an inefficient production. Despite the accuracy of the measurement not been presented in this study, it concludes that the procedure was able to control the deviation of sub-assembled sections making an important production improvement.

Ljubenkov, Zaplatic et al. (2008)used photogrammetry methods as a solution for the propulsion alignment of a ship when launched. In that work, it is presented a procedure in which measurements of the structure deflection in the machinery space and displacements of the main engine are taken before and after the launching. For that experiment there were taken 600 photos to capture 202 measuring points. After the launching, they succeed obtaining structure deflections up to 3 mm at the narrowest parts of the hull with an accuracy of 0.2 mm.

The results of a digital photogrammetric survey, performed on the 81-foot Italian Navy motor yacht “Argo”, were presented by Menna, Ackermann et al. (2009). 540 circular coded targets were uniformly positioned on the hull surface, and approximately 75 circular code targets were positioned on both the screw propellers. A 12 Mega pixels DSLR camera was used for the image acquisition. About 400 pictures of the boat surface and 60 images per screw propeller were taken with both parallel and convergent camera axes.

A photogrammetric approach for measuring weld-induced initial distortions in plated structures was presentedby Chen, Garbatov et al. (2010); Chen, Garbatov et al. (2011); Chen, Garbatov et al. (2011). Compared with initial imperfection classifications, a new

equation to predict the initial imperfections of very-thin-walled structures has been developed.

In the field of civil engineering, Jiang, Jáuregui et al. (2008)presented a literature review of close-range Photogrammetry applications in bridge deflection measurements. A list of experiences carried out from 1985 to 2003 was presented stating that most of them reached an order of accuracy of about 1mm. One of the experiences listed was presented by Whiteman, Lichti et al. (2002)in which two video-camera system were used to measure vertical deflections in a concrete beams during destructive test. Despite of the camera resolution not being as high as a photographic CCD, a precision of 0.25mm was reached, demonstrating the feasibility of obtaining measurements even with low-resolution video camera.

Dias-da-Costa (2011) presented a procedure based on Photogrammetry and image post-processing to measure surface displacements in laboratory test. The aim of that study was to overcome the drawbacks of the traditional methods of measurements. Among those drawbacks were the limitations in hardware positioning, the costs of the equipment and human resources; and time-consuming data processing, as it happens with Displacement-Transducers (LVDT). Therein, it was compared the results obtained by Photogrammetry methods with the measurements coming from LVDT elements. The results showed a high correlation between the values obtained from both systems. The coefficient of determination equals to 0.9994. Similarly, Bambach (2009)used a photogrammetric procedure to accurately capture the full surface transverse buckling deformations of the flanges and webs. In his work, he investigated edge-stiffened flanges structures numerically modelled and validated against the experimental results captured by photogrammetric procedures.

Luhmann (2010)presented a study summarizing recent developments and applications of digital Photogrammetry in industrial measurements. Therein it refers to new concepts for close-range Photogrammetry applications owing to the availability of video and digital cameras in combination with direct access to the digital image data generated. On one hand, off-line system scansare regarded as fully accepted 3D measurement tools that applied in a large variety of industrial application areas, yielding a typical measurement precision on the object in a range of 1:100000 to 1:200000 that is 0.1 mm for an object of 10 m size. On the other hand, on-line Photogrammetry systems have the capability of providing measurements in a real time, however, they are less accurate, approximately from 1:4000 to 1:10000.

To summarize, it can be stressed that after more than one hundred and fifty years of development, close-range Photogrammetry has been progressed sufficiently in terms of accuracy and practicability. Many experiences have been proven the potentialities of this technique in several fields and the current and quick progress of the cameras and computer processors, make this technology even more eligible modelling structures ensuring high accuracy results.

3. PHOTOGRAMETRIC MODELLING

Photogrammetry is an approach that can determine the size and the shape of objects through analysing images previously recorded by a photographic or video camera. Photogrammetry is divided in two differentiate techniques, analytical and digital. While the principal objective of the present work is to develop a model for the initial imperfection of plates, which is based on analytical Photogrammetry, there are some interesting advantages when using digital Photogrammetry, for example, in corrosion assessment.

The position of an object in space can be defined by a three-dimensional Cartesian co-ordinate system: the origin, the scale and the orientation of which can be arbitrarily defined. When having more than one photo, it is necessary to convert between co-ordinates in systems, what it is known as co-ordinate transformation. It can be divided into three parts: scale change, translation and rotation. The scale change along the three axis depends on the factor λ and may be represented by the vector equation $x = \lambda X$, where $X = [X\ Y\ Z]^t$ is the position vector of a point in the primary co-ordinate system and $x = [x\ y\ z]^t$ is the position vector of the point in the scaled co-ordinate system. As for the translation of axes, they may be represented by the following vector equation: $x = X - X_0$, where X is the position vector of a point, in the primary coordinate system, $X_0 = [X_0 Y_0 Z_0]^t$ is the position vector of the origin of the secondary coordinate system, relative to the primary coordinate system and $x = [x\ y\ z]^t$ is the position vector of the point in the secondary co-ordinate system. The rotational process may be expressed as a result of the three independent sequential transformations, correspondent to each axis. For a given point, called A, in a coordinate system (x, y, z), if a rotation $\omega, \varphi\ and\ k$ is made clockwise about all the axis, the position vector of A in the rotated system$(x_{w\varphi k}\, y_{w\varphi k}\, z_{w\varphi k})$ system will be $[x_{w\varphi k}\, y_{w\varphi k}\, z_{w\varphi k}]^t = R_w R_\varphi R_k\ [xyz]^t$.

The basic concept for building a functional model in a close range Photogrammetry is the central perspective projection. Being a point called a, three-dimensional positioned point in the space, and its projection onto the *projection plane*, it is defined as a straight line passing through AO, where O is the perspective centre. At the same time, it defines the straight line POP as an orthogonal one to the projection plane and the distance OP as the *principal distance* denoted as C.

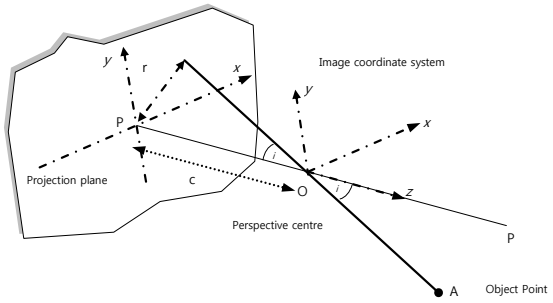

Figure 2 Central perspective projection

In order to derive the functional relationships between the position of the object A and its projection on the *projection plane*, two co-ordinate systems may be introduced. The primary system $(X\ Y\ Z)$ is arbitrarily located in the object space. In this system, the coordinates of the perspective centre of the secondary system are $(X_0 Y_0 Z_0)$, and the coordinates of the point A are $(X_A Y_A Z_A)$. The secondary system $(x\ y\ z)$ has its origin in O, where the perspective centre is. The z-axis coincides to the orthogonal lines POP, and the x-axis and y-axis are parallel to the ones from the *projection plane.* Once both coordinatesystems are defined, it is possible to write the vectors relative to the primary coordinate system: $X_A = X_0 + S$ where S is the position vector of A relative to O. It is collinear with x_a but in opposite sign:

$$X_A = X_0 - \mu R^t x_a \tag{7}$$

in matrix notation:

$$\begin{bmatrix} X_A \\ Y_A \\ Z_A \end{bmatrix} = \begin{bmatrix} X_0 \\ Y_0 \\ Z_0 \end{bmatrix} - \mu \begin{bmatrix} \gamma_{11} & \gamma_{12} & \gamma_{13} \\ \gamma_{21} & \gamma_{22} & \gamma_{23} \\ \gamma_{31} & \gamma_{32} & \gamma_{33} \end{bmatrix} \begin{bmatrix} x_a \\ y_a \\ -c \end{bmatrix} \tag{8}$$

where μ is a scalar quantity, greater that zero and γ_{ij} are elements of the rotation matrix R.

If now it is considered the same relationship, but this time expressing the primary coordinate system to the secondary one, it is obtained the reverse transformation:

$$x_a = \mu^{-1} R(X_0 - X_A) \tag{9}$$

in matrix notation

$$\begin{bmatrix} x_a \\ y_a \\ -c \end{bmatrix} = \mu^{-1} \begin{bmatrix} \gamma_{11} & \gamma_{12} & \gamma_{13} \\ \gamma_{21} & \gamma_{22} & \gamma_{23} \\ \gamma_{31} & \gamma_{32} & \gamma_{33} \end{bmatrix} \begin{bmatrix} X_0 - X_A \\ Y_0 - Y_A \\ Z_0 - Z_A \end{bmatrix} \tag{10}$$

where the third equation can be explicitly written byμ^{-1} resulting in the following equations:

$$x_a = \frac{-c\,[\gamma_{11}(X_0 - X_A) + \gamma_{12}(Y_0 - Y_A) + \gamma_{13}(Z_0 - Z_A)]}{[\gamma_{31}(X_0 - X_A) + \gamma_{32}(Y_0 - Y_A) + \gamma_{33}(Z_0 - Z_A)]} \tag{11}$$

$$y_a = \frac{-c\,[\gamma_{21}(X_0 - X_A) + \gamma_{22}(Y_0 - Y_A) + \gamma_{23}(Z_0 - Z_A)]}{[\gamma_{31}(X_0 - X_A) + \gamma_{32}(Y_0 - Y_A) + \gamma_{33}(Z_0 - Z_A)]} \tag{12}$$

In digital Photogrammetry (DP), the photos are taken in a paired stereo configuration and the object's surfaces appearing in them should be of certain characteristics, being the most important its texture and reflective surfaces induce inexact results. Due to its aim, DP can be thought of as camera-based 3D 'Laser-Scanner'. In fact, both systems generate DSM and each one shows some lights and drawbacks depending on the projects to be studied. A deeper comparisons of both systems may be found in (Zaplatic 2008).

Dense Surface Modelling is based on an algorithm that searches for image patches that 'look' alike from an existing oriented project composed of stereographic photographs. When a good match is found between two photographs, the orientation and camera data allows the program to compute the correct 3D location of the surface point corresponding to the image patch (Inc 1992-2008).

4. SURFACE FITTING

The measurements taken from the photogrammetric techniques are used to generate mathematical functions. This function may be utilized to generate the models of the plates. The reason of using mathematical functions instead of directly using the mesh obtained from photogrammetric techniques relies on the fact that the important information to be considered into the structural analysis is rather the trend of the shape than the plate particularities. It means that the data is filtered and smoothed. Moreover, the straight exchange of mesh data between software often causes erroneous results due to incompatibilities between software.The method used to generate such mathematical functions is based on third polynomial functions.

The initial problem can be defined as follows: given N data points (x_i, y_i) and N numbers $f_i, i = 1,2,\dots,N$, find a function $f(x,y)$ from some class and defined on a plane containing the data points for which $f(x_i, y_i) = f_i$ for $i = 1,2,\dots,N$. A class is defined as the polynomial function of the same order in both x and y and the first four ones are as follows.

Table 2 Polynomial Classes

Class	Basis Function
$\mathcal{P}_0$	1
$\mathcal{P}_1$	1 x y
$\mathcal{P}_2$	1 x y x^2 xy y^2
$\mathcal{P}_3$	1 x y x^2 xy y^2 x^3 x^2y xy^2 y^3

As a result of any fitting, there is a difference between the original coordinates of a point and the coordinates obtained from the calculated function (Lancaster and Salkauskas 1987). This difference is defined as $p(x_i, y_i) - f_i$. The objective is then to adjust p by choosing the coefficients $a_0, a_1, a_2, \dots, a_n$ so as to minimize,

$$E(p) = \sum_{i=0}^{N} (p(x_i, y_i) - f_i)^2 \tag{13}$$

E is a function of$a_0, a_1, a_2, \dots, a_n$and will have a minimum only when $\frac{\partial E}{\partial a_i} = 0$ for $i = 1,2,\dots,6$. These conditions yield to six linear equations of the unknowns $a_0, a_1, a_2, \dots, a_6$.As for the case of a higher function's class, more coefficients are involved, as it is the case of the cubic functions:

$$p(x,y) = a_1 + a_2 x + a_3 y + a_4 x^2 + a_5 xy + a_6 y^2 + a_7 x^3 + a_8 x^2 y + a_9 x y^2 + a_{10} y^3 \tag{14}$$

Since the number of points composing a project of surface modelling might be of well over 100, it is necessary to call on computer tools. To proceed in finding the coefficients that minimize the difference $p(x_i, y_i) - f_i$, it is used Matlab.

The polynomial degree to be used depends on the complexity of the plate shape to be modelled. If the shape is totally flat, a fitting of first order in both x and y axis would be enough. However, if the plates were fully wavy, it would be necessary to use a higher order. The higher degree allows a more complex shape, nevertheless, the use of higher polynomial degree will involve an increase of the number of coefficients, and hence, the computational efforts. Furthermore, higher degrees functions generate more wavy surfaces, and that could generate erroneous shapes, especially on the borders and corners.

The dimensions of the specimens studied in here have an aspect ratio a/b = 2 approximately. Thus, it is expected not to observe more than two half waves in the longitudinal axis, so at least third polynomial degree is necessary. To study the fitting behaviour of several polynomial degrees functions, it has been performed series of fittings, starting from the first degree until the fourth one. The order has been increased for both x and y axis separately. From each fitting has been calculated the correlation between the surface generated and the photogrammetric points. The goal is to study when the increase of the coefficients is not compensated with a gain of correlation.

Figure 3represents the trend of the coefficient of determination (R-square) performed for all the plates studied and in the Table 3 shows the resultant R-square of each case. The trend is drawn by a surface of the second order. It can be observed that the R-square increases while the degree in each axis increases. Despite the surface appearing to decrease, when the degree reaches the third order, the R^2 obtained is of the same magnitude, meaning that for plates of a/b=2 third order polynomialsare enough to faithfully model their shapes.

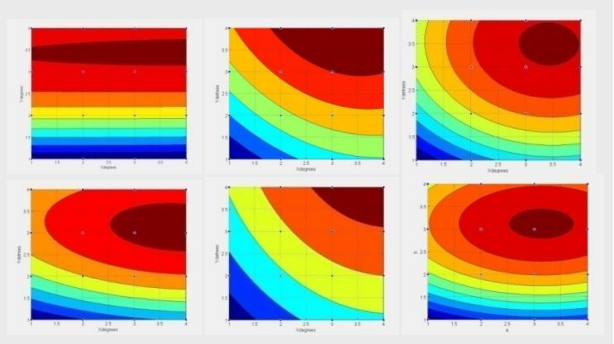

Figure 3 Correlation of fittings of different degrees

Table 3shows the coefficient of determination. Only in one case, it has been observed a considerable improvement of the adjusted R-square, corresponding to the stiffened plate number 7. Matlab is

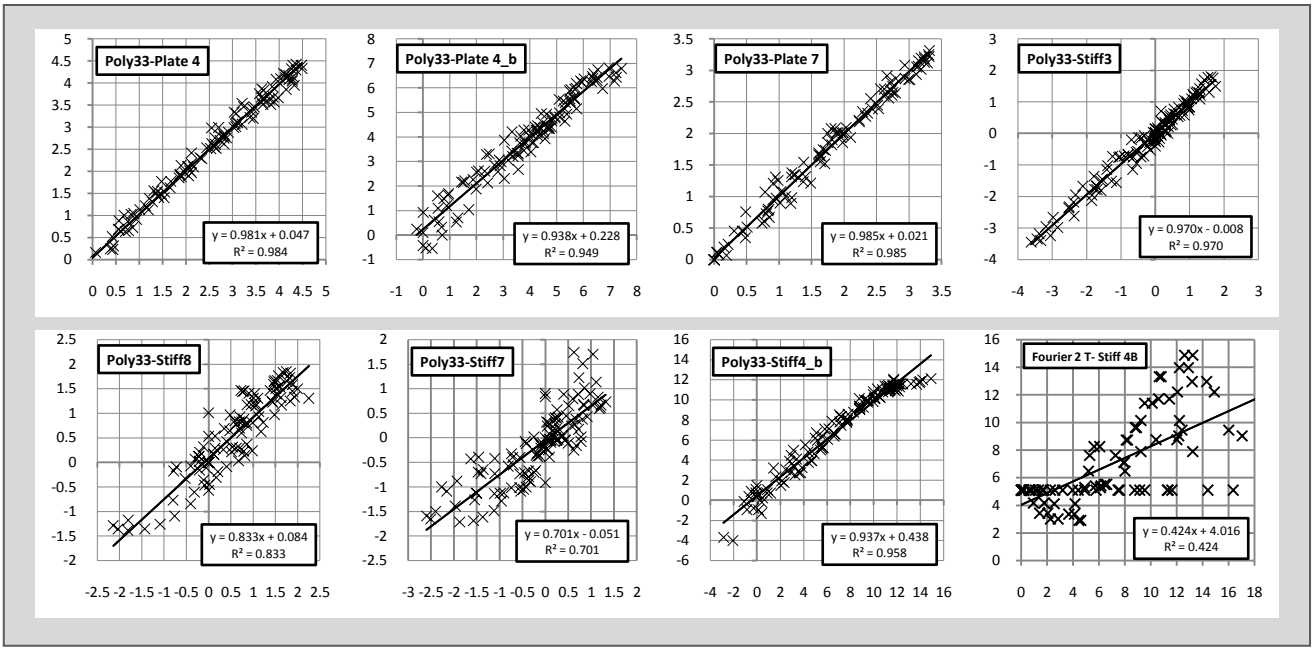

Figure 4 Correlations of the third degree polynomial and Fourier (2 terms) functions

used to compute the ten coefficients corresponding to the fourth class of polynomials and it has been found that while un-stiffened plates are better adjusted with only one-half wave, the stiffened plates demonstrate higher irregular shapes.

Table 3 R-square of the Polynomial and Fourier functions

X Deg	Y Deg	Pl. 4 B	Pl 4 L	Pl. 7	St. 3	St. 4 B	St.7	St. 8
1	1	0.22	0.08	0.09	0.55	0.19	0.06	0.61
2	2	0.81	0.97	0.92	0.81	0.76	0.56	0.71
3	3	**0.95**	**0.98**	**0.98**	**0.97**	**0.96**	**0.68**	**0.81**
4	4	0.97	0.99	0.98	0.98	0.97	0.83	0.85
Fourier model		0.54	0.67	0.73	0.15	0.49	0.04	0.04

The correlations of the third order polynomials for all the plates are plotted in the Figure 4. Some plates are better represented than others, and that is caused by the distortions from the dominant shape that are found in some case, for example, the stiffened plate number 7. The lower correlations correspond to those cases where the amplitude of the initial deformations is small. Contrarily, if the initial deflections are more evident, the correlation improves. In the same sense, if the plate is extremely deformed, the third order polynomial face some difficulties to represent the upper values, as it may be seen in the case of the Stiffened 4B plot, where a trend is visible in the upper values.

Furthermore, a comparison with the trigonometric models is carried out. The amplitude of the Fourier terms is calculated using the Custom Function tool from Matlab that finds the coefficients that minimizes the residuals. The last row of the Table 3shows the R-square obtained from the fittings carried out using the Fourier series of 3 terms for the longitudinal direction. In addition, the correlation of a Fourier model of two terms has been performed for the case Stiffened plate 4B and is represented in the last plot of the Figure 4.

According to the R-squares obtained by Fourier models it may be concluded that these models fit better to un-stiffened plates, and that is because the dominant shape correspond to the first mode of deformations, on the other hand, very low results are attained in the stiffened plates, besides the Stiffened 4B that also presents an evident overall deformed shape.

5. SENSITIVE ANALYSIS

Despite the fact the accuracy of the photogrammetric measurements may be calculated mathematically, some tests are carried out to prove the correlation between the results and the actual measurements. To do so, three tests are performed; the first one consists in making a plaster cast of a plate. Using a plaster cast permits to take measurements of the out-of-plane distortions by drilling the cast. In the second test, measurements of a very deformed plate (Stiffened 4B) are taken from a quasi-perfect plate.The plate to study and the quasi-perfect plate are faced one to each other, and since the quasi-perfect plate is drilled, a calliper may be used to take measurements. The third test consists in dispose of 161 points over a surface that is as much flat as possible. The goal is to check out if Photogrammetry is able to catch such flatness. The results of the test draw high correlated values, an R-square from 0.938 up to 0.998. However, it should be considered that some deviations may be attributed to the inaccuracies of taking measurements or the difficulty of generating absolutely perfect flat planes.

Table 4 GOF of the tests

	SSE	Mean	SSR	SST	ST.DV	R^2
Test 1a	12103	6.72	1845	1965.6	1.17	0.9384
Test 1b	97.14	6.72	1694	1790.9	1.05	0.9458
Test 1c	76.73	5.27	2233	2309.3	0.94	0.9637
Test 1d	89.60	5.24	2242	23315	1.01	0.9582
Test 2a	0.31	0.02	53	53.4	0.05	0.9946
Test 2b	0.15	0.00	61	61.2	0.04	0.9975
Test 3	9.86	84.44	184061	184070.8	0.25	0.9999

6. STUDY CASE

In order to carry out the strength assessment of plates it has developed a methodology that integrates all the steps involved in the analysis. The procedure that is represented in Figure 6 is mainly composed by three stages that are coincident with three dusting techniques: Photogrammetric modelling, Surface Fitting, and Finite Element Analysis.

The methodology is designed in such a way all the data involved in the procedure are suited properly and managed in a way it might be used in the following stages. The whole procedure is done straight skipping redundant steps, making it quicker and more reliable.

6.1. Stage 1: Photogrammetry

To solve the analytical photogrammetric equations, a commercial code called Photo-modeller has been used. This program helps in extracting measurements and 3D models from photographs, by

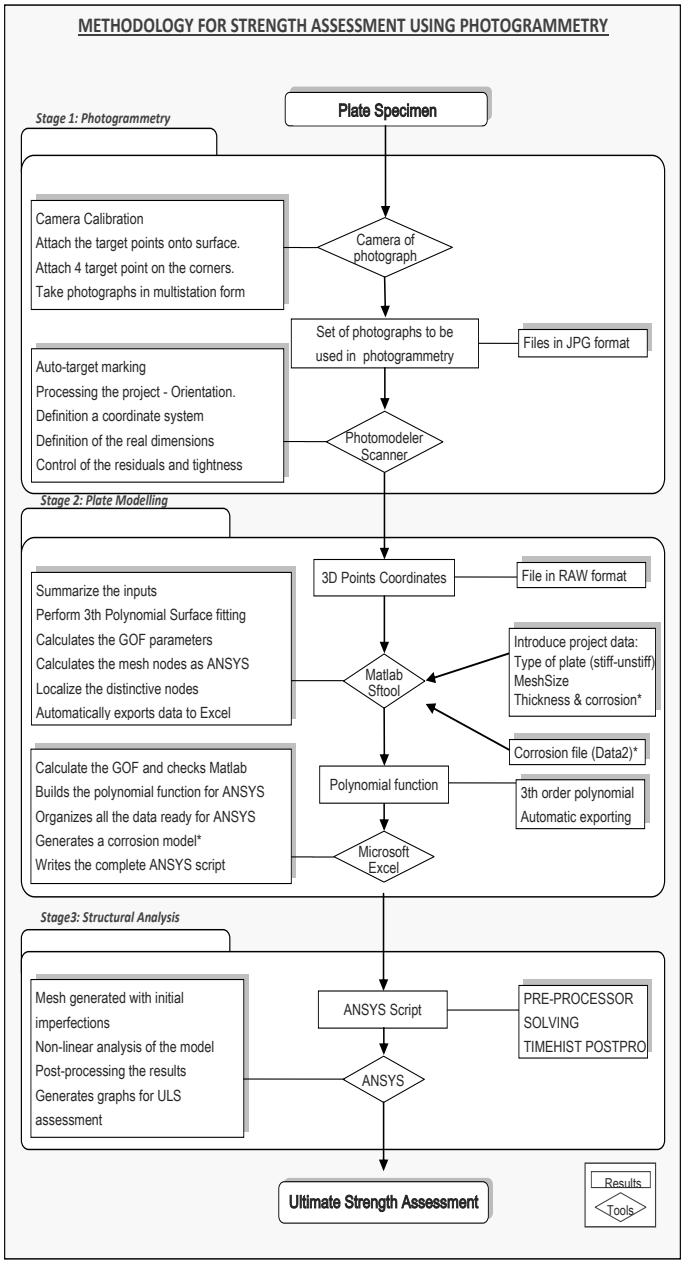

Figure 6 Scheme of the Methodology

using a camera as an input device. The model can be created automatically by using auto referencing marking codes with the so-called *Automatic Target Marking*. This procedure is used to model the plates since it is more reliable and faster than manual one. On the other hand, asub-program called Photo-modeller Scanner is aimed to create models by using stereographic photos. Thissub- program has been used to estimate the level of corrosion of the plates.

The camera used in this study is a Sony Alpha 100, which is able to shoot photos up to 10 Megapixels, this permits to work far over the minimum recommended of 2 Megapixel. Before starting with any project, it is necessary to calibrate the camera and the lens under the conditions that are going to be used such as the focal length. The quality of the results obtained in the project depends very much on the quality of the calibration.

The objective is to model the deflections of the plates, and the way to do is by attaching reference points onto the surface of the plates, following the shape. These reference points are known as *coded target points* and they are physical codified points whose the program is able to find inside of a photograph. In order to ensure that the target points follow the shape of the plates with more fidelity, the targets might be disposed in magnetic strips

From the solution of the collinearity equations, the program is able to measure the accuracy of the project by measuring the distances between the expected point coordinates and the ones observed in the photographs, that is, the residuals. There is one computable residual for each point in each photograph. For a project to be considered of high accuracy, the maximum residual reached should not be larger than 1 pixel.

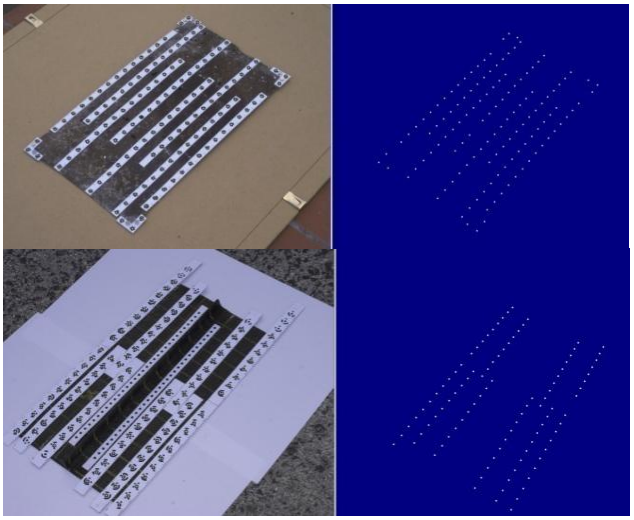

Figure 5 Plate modelling, showing target points.

Table 5 shows the qualitative values of the projects carried out with Photo-modeller. In 5 cases, 8 photos are taken per plate and in two cases, only 4 photographs were considered to be used attaining the same order of accuracy. Figure 5 shows two examples of point of clouds representing the plates.

The results of the photogrammetric stage are the coordinates of a set of points that represents the surface of the plate. These coordinates are saved in a RAW file that is used to generate the polynomial functions that will be utilized to generate the model.

6.2. Stage 2: Plate modelling

A proposal to systematize the procedure for generating a script to run in the finite element code software (ANSYS) is presented in here taking into account the data of the plate and some other parameters that are necessarily to be defined. ANSYS scripts may be created automatically by using two programs, Matlab and Excel. The starting point of designing this procedure is to define what data is required to carry out a finite element analysis and how it must be organized.Figure 7 shows all data necessary to proceed and the sequence of its use through all the programs.

Table 5 Qualitative values of the projects

Name	Nº Ph.	Coverage	Overall RMS	Max RMS	Min RMS
			mm		
Stiff 8	8	89%	0.022	0.033	0.022
Stiff3	8	89%	0.059	0.081	0.057
Plate7	8	88%	0.027	0.029	0.026
Plate4	8	89%	0.019	0.021	0.019
Stiff7	8	89%	0.018	0.021	0.017
Plate4_B	4	89%	0.034	0.092	0.029
Stiff4_B	4	89%	0.015	0.025	0.014

A macro in Matlab is written to automatically carry out a third polynomial surface fitting and to calculate the polynomial coefficients based on the points' coordinate computed by Photo modeller. The macro also calculates the mesh size about the number of nodes in X-axis and generates an array with nodes that will be further created by ANSYS pre-processor and their coordinates, named Data1.

All the data generated by Matlab is stored automatically in an Excel's file. This file is previously designed in such a way is able to read the data stored by Matlab and generate a script file to be run with ANSYS program.

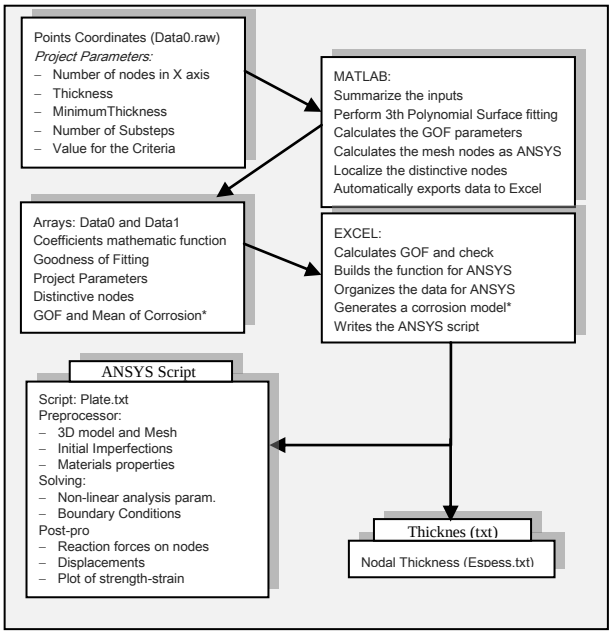

Figure 7 Data flow

6.3. *Finite Element Analysis*

The plates are modelled by nonlinear shell elements SHELL181 of four nodes and each node having 6 degrees of freedom. This type of element permits to set up non-linear and multi-linear material properties. The nonlinear material properties are defined as MISO, that is, multi-linear isotropic hardening and three points are defined as zero stress-zero strain; yield point/young modulus-yield point and 0.2-ultimate strength. As for the mesh size it has been studied the convergence when refining the mesh and it has been concluded that the model converges monotonically and that no significant improvement is obtained for meshes more refined those 1000 nodes.

The analysis based on two modelling procedures. On one side, the model is deformed considering the measurements taken from Photogrammetry and on the other side, the model is deformed taking into account the trigonometric deformations with a maximum amplitude of $w_0 = 0.12\,\beta^2$ as proposed by Antoniou (1980). The first specimens to be analysed are the un-stiffened elements Plate 4, Plate 4B (Figure 10) and Plate 7 (Figure 9).

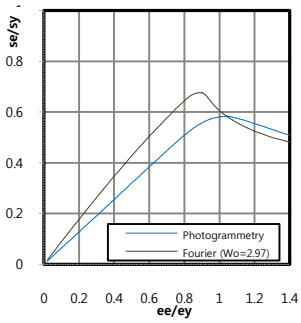

Figure 10Stress-strain,unstiffened plate 4B

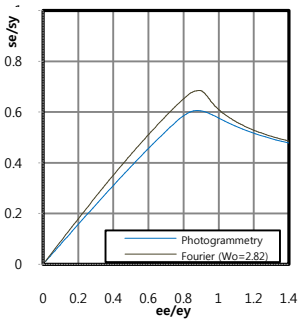

Figure 9Stress-strain, unstiffened plate 7

Initially the plates are considered not to be affected by the corrosion. As it was expected, the deformations induce a decrease of the load carrying capacity of the plates and the ultimate strength is reduced to the half of the yield stress approximately. As it can be seen, in the two cases represented the UTS reached in the models deformed using Fourier functions are slightly higher than the ultimate strength capacity attained in the models based on the photogrammetric measurements.

When studying the stresses and the deformation of the plates in more detail it may be observed some differences between the two types of modelling. As an example, the behaviour of the Plate 4B is studied in more detail.

Figure 8a plots the $z-axis$ deformation Figure 8b, the Von Misses stresses on the plate modelled using the Fourier functions, both correspond to the moment at which the ultimate strength is reached. It is appreciable that there is symmetry in both axes. This symmetry is found from the beginning of the load application up to the UTS, and after this point, the plate behaves asymmetrically. On the other sideFigure 8c and Figure 8d show the deformations of the $z-axis$ and Von Mises stresses respectively of the plate modelled using the photogrammetric measurement. In this case, it is not observed the symmetry seen before and consequently, a decrease of the strength is observed. Furthermore, the strain at which the UTS may vary depending on the level of asymmetries.

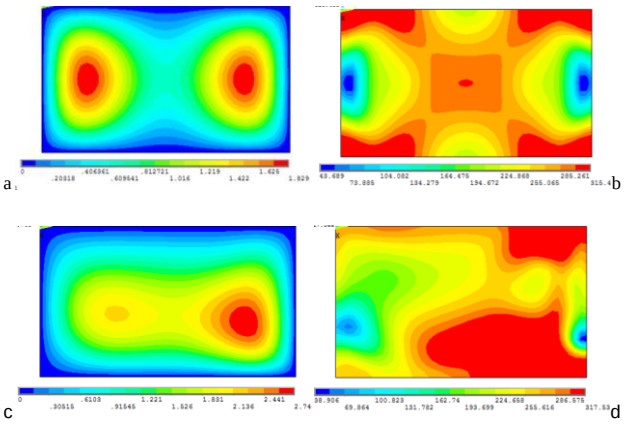

Figure 8Plate 4B deformation

Similar procedure has been used with the stiffened plates. Because of the presence of the stiffener attached to the plate and due to the fact that the boundary conditions are different, the results obtained are expected to be different. Attending to the graphs, it is appreciable that stiffened specimens 4, 7 and 8 perform similarly while the stiffened plate number 4B behaves in a different manner. This is because of the fact that the initial deformations of the specimen 4B conduce to a very early plate overall buckling.

It has been seen that asymmetries cause a strength reduction in un-stiffened plates, however, in stiffened plates the asymmetries may cause a rise of the ultimate strength compared to the values obtained with the Fourier models.

Attending to the plots of displacement it may be easily seen that the plates are influenced not only by the slenderness but also by the shape of the initial deformations. Within the pre-buckling part, the initial imperfections are amplified once the load is applied and as the buckling capacity is approached, the plate gradually changes the shape in order to adopt its lowest energy shape. In the case of the Fourier models, the initial dominant shape is one-half sine wave while the lowest energy corresponds to two half-sine waves. The transition from the first shape to the other is done in a short piece of time and consequently the strength-strain curve presents a sharp slope change.

On the other hand, the models analysed using photogrammetric measurements present asymmetries in both axis similarly to the un-stiffened plates. These asymmetries are found to be very influential in the behaviour for mainly two reasons. The first reason is related to the lowest energy shape, that, while in the models done with Fourier functions are found to be of two-half sine waves, in the photogrammetric models are of different shapes

in each case. As an example, Figure 11and Figure 12 show the shapes of the plates 3 and 8 at the ultimate strength capacity. The plots on the left correspond to the plate modelled using trigonometric Fourier functions while the plots on the right show the model based on photogrammetric measurements.

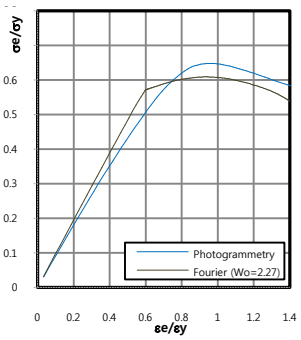

Figure 14Stress-strain,stiffened plate 3

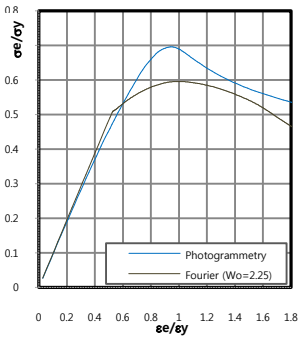

Figure 15Stress-strain, stiffened plate 7

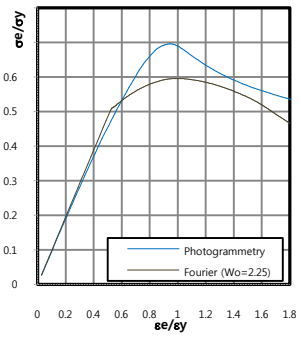

Figure 17Stress-strain, stiffened plate 8

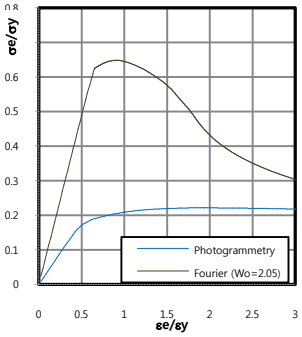

Figure 16Stress-strain, stiffened plate 4B

As it can be seen, the displacements of the Fourier models are symmetric and the lowest energy shape has been found always to correspond to the second mode of deformation that is of two-half sine waves. On the other hand, the shape of the photogrammetric models at the ultimate strength point may adopt various forms, being dominated by the initial out-of-plane deviations, and because of that, the strength varies in each case.

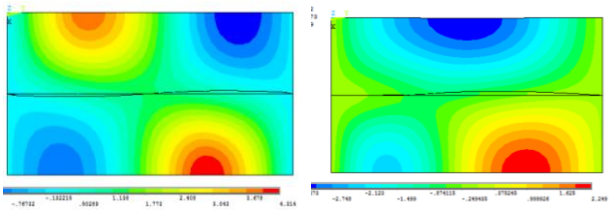

Figure 11Displacements at UTS of Stiff 3, Fourier (left) and Photogrammetric (right) model.

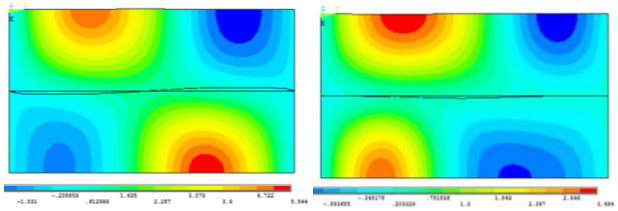

Figure 12Displacements at UTS of Stiff 8,Fourier (left) and Photogrammetric (right) model.

The second reason is related to the transition of the shapes that plates adopt. Since the initial distortions of the photogrammetric models are more dominant than the one of Fourier cases, the plates do not perform any transition, and thus, there is no any sudden change of the strength-strain curve slope. Evidently, the asymmetries observed in the displacements may be seen in the von Misses stresses. Figure 13represents a stress distribution of the stiffened plate 7when the ultimate strength is reached.

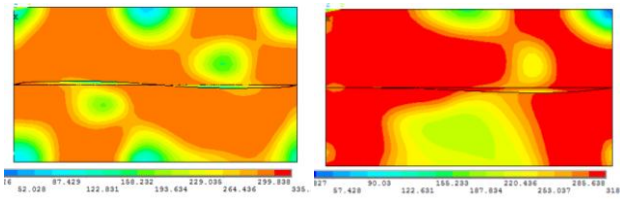

Figure 13 Stresses of plate Stiff 7, Fourier (left) and Photogrammetric model (right)

7. CORRODED PLATES

Apart from initial imperfections modelling based on analogicalPhotogrammetry, it has been carried out an analysis with which the corrosion is modelled using the digital Photogrammetry. This procedure has been done using the specimen stiffened 4B, that has been treated as an un-stiffened plate. Using Photo-modeller, it has been created a cloud of points following the surface roughness from photographs, having this cloud the corrosion may be computed. The digital Photogrammetry is able to detect not only the trend of the shape but also the roughness of the surface in very small details. Knowing the roughness, as well as the location of each node of the finite element model it is possible to determine the corrosion characteristics corresponding to any particular node.

To make a comparison of the results, three simulations based on three different models of corrosion degradation are carried out. The first model considers the plate without any corrosion and the thickness has been set up of 2.9 mm; the second, takes into account the corrosion, modelled using digital Photogrammetry where the mean value thickness is about 2.61mm, the standard deviation is 0.0964 mm and the COV is 0.037; the third model is randomly corroded by using the same parameters obtained from Photogrammetry, that is, the mean value thickness of 2.63 mm, standard deviation 0,097 mm and COV 0,037. All the models have been deformed using Fourier functions with amplitude of $Wo = 2.05$ and the results are shown in the Figure 18.

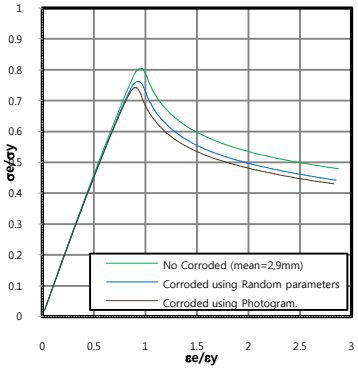

Figure 18 Corrosion modelling, stress-strain of plate 4B

It can be observed that despite the statistical values of the two corrosion types modelling to be the same, the plate behaves slightly different. Figure 19 shows the displacements of the plate and the stresses at UTS of the random distributed corrosion model and Figure 20 the corroded model using the photogrammetric data. It is observed that the displacements and stresses in the photogrammetric model are more irregular compared to the random distributed model. The displacement figures also show that in the case of the random distributed model the plate reaches the maximum load carrying capacity being more symmetric than the photogrammetric model.

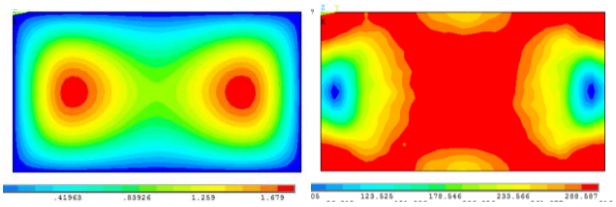

Figure 19 Displacements (left) and tresses (right), Random corroded surface model

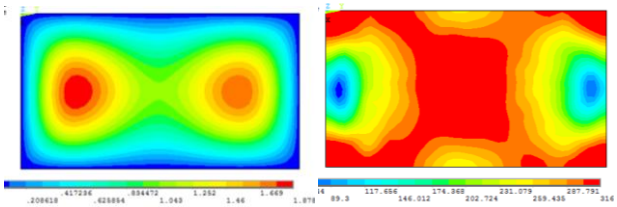

Figure 20 Displacements (left) and stresses (right), Photogrammetric corroded surface model,

8. DISCUSION

The Table 6 shows the ultimate strength of plates based on different initial imperfection models: modelled using Fourier functions and modelled using polynomial functions from photogrammetric measurements. Apart from the case of the stiffened plate 4B, the un-stiffened plates showed more optimistic UTS in the models based on Fourier functions while in the stiffened plates more optimistic results are obtained from the photogrammetric ones.

The results obtained from the photogrammetric models are more variant and even in one case -stiffened 4B- the results are completely different from the Fourier models. This is owed to the fact that models based on Photogrammetry consider the geometrical particularities of each plate that might be deformed in a different manner than the others.

Table 6 Ultimate Strength of the plates

Name	Thickness	β	ϕuF/ϕy	ϕuPH/ϕy
Plate4	2.70	2.5	0.78	0.74
Plate4_B	2.01	3.5	0.68	0.58
Plate7	2.02	3.4	0.68	0.61
Stiff3	2.90	2.6	0.61	0.65
Stiff4_B	2.90	2.4	0.65	0.22
Stiff7	2.50	2.7	0.60	0.70
Stiff 8	2.22	3.3	0.50	0.55

When comparing the behaviour of un-stiffened plates modelled with Fourier and Photogrammetric basis, the following conclusions may be drawn:

- The initial deformation of the un-stiffened plates, modelled by the Photogrammetry, is similar to those generated by the trigonometric Fourier functions. The initial mode of deformation is found to be the same, the first mode. However, despite both models being more alike than the case of stiffened plates, two singularities are still remarkable: the small asymmetries that are not considered in Fourier models and the out-of-plane borders. These singularities and the fact that the initial amplitude is not the same bring the results to be different.
- The difference in strength between the two modelling types is approximately of 10% in the studied cases. The lower values obtained for the photogrammetric models might be induced by the asymmetries found in those models.
- The more differentiate strength-strain curve corresponds to plate 4B, that it is found to be the more asymmetrical shape of the plate modelling stage. The differences are found not only in the ultimate strength but also in the strain that it is reached.

From the comparison between the behaviour of stiffened plates modelled with the Fourier and Photogrammetric basis, the following conclusions may be drawn:

- The strength-strain curves obtained from models done with Fourier functions and Photogrammetric models are slightly different in terms of the shape as well as the ultimate strength is reached.
- In the case of the un-stiffened plates, the asymmetries cause an ultimate strength reduction when compared to the Fourier models. On the other hand, it seems to provoke a strength improvement in the case of stiffened plates. Such effect might be caused by the opposition of the initial imperfections to the lowest energy configuration shape, strengthen to specimen.
- In one case, stiffened plate 4B, the plate is initially very deformed and plate-induced overall buckling is easily identifiable. Such imperfections bring the specimen to lose its load carrying capacity very early. This eventuality is a proof that the photogrammetric strength assessment ensures a more accurate knowledge of the real strength capacity of plates.

Finally, from the procedure of corrosion modelling, the following conclusions may be outlined:

- The digital photogrammetric procedure is able to catch the distribution of the corrosion depth along the surface of the plate. If it is the case that in some parts of the plate the degradation of the plate is more severe, then, the plate may lose its strength capacity due to these particularities and may induce an asymmetrical deformation. In the example carried out in this work, such asymmetries have been detected in the photogrammetric model, which leads to the loss of its load carrying capacity earlier than the one modelled by the use of random parameters.

9. CONCLUSIONS

In this thesis, a new approach has been developed, based on photogrammetrictechniques that allow the generation of surface models taking into account the real shape of the plates.

This approach involves several steps that are identified and organized in such a way so that the strength assessment may be carried out in an easy and reliable manner. The procedure is mainly composed of three stages that are coincident with three dusting techniques: Photogrammetric modelling, Surface Fitting, and Finite Element Analysis. In order to achieve the final objective, it proposes a methodology that integrates the three techniques. This methodology is designed in a way that the accuracy is maximized while the number of the steps and the time is minimized.

Based on this methodology, the faithful geometry models of seven plates, three un-stiffened and four stiffened ones, originally belonging to a box girder were analysed. These models have been used to carry out finite element analysis. The results obtained are used to perform some comparisons between the photogrammetric models of initial imperfection and other types of modelling. It has been proved that photogrammetric models are able to catch the asymmetries present in the real plates. In the structural analysis it has been found that such asymmetries are very influential to the plate configuration at which UTS is reached and hence, the maximum carrying capacity is noticeably affected.

Finally, it has been presented a procedure to study the corrosion of plates by using the digital Photogrammetry. This procedure that relies on stereographic consists in computing the degradation with regard of the dispersion of the cloud of points generated by the digital Photogrammetry. This procedure has allowed detecting the real distribution of the corrosion degradation along the plate and as a result, different behaviour has been observed.

10. REFERENCES

Antoniou, A. C. (1980). "On the maximum deflection of plating in newly built ships." Journal of Ship research**24**(1): 31-39.

Bambach, M. R. (2009). "Photogrammetry measurements of buckling modes and interactions in channels with edge-stiffened flanges."Thin-Walled Structures**47**(5): 485-504.

Carlsen, C. A. (1977). "Simplified collapse analysis of stiffened plates. ."Norwegian Maritime Research**5**(1-4): 135-177.

Carlsen, C. A. (1978). "The specification of post-welding Distortion Tolerances for Stiffened plates in compression." The Structural Engineer**56A**(5): 133-141.

Chen, B., Y. Garbatov, et al. (2010). Displacement Measurement of Box Girder Based on Photogrammetry. Proceedings of the 11th International Symposium on Practical Design of Ships and other Floating Structures (PRADS 2010), paper PRADS2010-20083, Rio de Janeiro, Brasil, Aped - Apoio e Produção Ltda.

Chen, B. Q., Y. Garbatov, et al. (2011). Automatic Approach for Measuring Deformations in Complex Structures Using Photogrammetry Technique.Proceedings of the XXII Pan American Conference of Naval Engineering, Maritime Transportation & Ports Engineering, Buenos Aires, Argentina.

Chen, B. Q., Y. Garbatov, et al. (2011). "Measurement of weld induced deformations in three-dimensional structures based on photogrammetry technique." Journal of Ship Production and Design**27**(2): 51-62.

Chi, L. E. W., G. Y. Grondin, et al. (2006)."Interaction Buckling Failure of Stiffened Steel Plates."University of Alberta - Department of Civil &EnvironmentalEngineering(Structural Engineering Report No. 264).

Cui, W. a. M., A. (1988)."Effects of Welding distortions and residual stresses on the ultimate strength of long rectangular plates under uniaxial compression."Marine Structures**11**(6): 251-269.

Dias-da-Costa, D., J.J.Valença, Eduardo N. B. S. (2011)."Laboratorial test monitoring applying photogrammetric post-processing procedures to surface displacements."Measurement**44**(3): 527-538.

Dowling, P. J. and P. A. Frieze (1977)."Ultimate Load Behaviour of Plates in Compression."Steel plated Structures: International symposium [London 1978]. Ed by P.J. Dowling, J.E. Harding and P.A. Frize.**Chap. 2**: 24-50.

Faulkner, D. (1975). "A Review of Effective Plating for use in the Analysis of Stiffened Plating in Bending and Compression." Journal of Ship Research**19**: 1-17.

Frankland, J. M. (1940). "The strength of Ship Plating under edge compression."U.S Experimental Model Basin Progress Report**469**.

Guedes Soares, C. (1988). "Design Equation for the Compressive Strength of Unstiffened Plate Elements with Initial Imperfections."Journal of Constr. Steel Research**9**: 287-310.

Guedes Soares, C. (1988). "Uncertainty Modelling in Plate Buckling."Structural Safety**5**: 17-34.

Guedes Soares, C. and J. M. Gordo (1996). "Compressive Strength of Rectangular Plates Under Biaxial Load and Lateral Pressure." Thin-Walled Structures**24**: 231-259.

Inc, E. s. (1992-2008). "Photomodeler Scanner Tutorials."

Jiang, R., D. V. Jáuregui, et al. (2008). "Close-range photogrammetry applications in bridge measurement: Literature review." Measurement**41**(8): 823-834.

Kamiski, M. L. and J. Amdal (2000). "Ultimate Strength" Proceeding of the 14th International Ship and Offshore structures congress 2000, Japan**Volume 1**: 68.

Karman, T. V. and E. E. Sechler (1932)."The strength of thin plates in compression."Transactions of AS;E**54**: 53-57.

Koelman, H. J. (2010). "Application of a photogrammetry-based system to measure and re-engineer ship hulls and ship parts: An industrial practices-based report." Computer-Aided Design**42**(8): 731-743.

Lancaster, P. and K. Salkauskas (1987)."Curve and Surface Fitting."Harcourt Brace Jovanovich, Publishers.

Ljubenkov, B., T. Zaplatic, et al. (2008). "Measurements for reliability of ship design, production and operation interaction."

Luhmann, T. (2010). "Close range photogrammetry for industrial applications." ISPRS Journal of Photogrammetry and Remote Sensing**65**(6): 558-569.

Menna, F., S. Ackermann, et al. (2009).Digital Photogrammetry: A Useful Tool For Shipbuilding Applications. Proceedings of the 13th Congress of International Maritime Association of Mediterranean, IMAM, Istanbul, Turkey.

Smith, C. (1979). "Compressive strength of welded steel ship grillages."Trans RINA**117**: 325–359.

Smith, C. S., P. C. Davidson, et al. (1988). "Strength and Stiffness of Ships' Plating under In-plane Compression and Tension."Transactions RINA**130**: 277-296.

Whiteman, T., D. D. Lichti, et al. (2002)."Measurements of Deflections in concrete beams by close-range digital photogrammetry."

Zaplatic, T. (2008)."Dimensions and Shape Control of Sub-assembled Sections using Digital Photogrammetry."